Eur. Phys. J. Special Topics **222**, 47–60 (2013)

DOI: 10.1140/epjst/e2013-01825-0

THE EUROPEAN PHYSICAL JOURNAL SPECIAL TOPICS

Regular Article

Protein adsorption and interfacial rheology interfering in dilatational experiment

P.A. Rühs[a], N. Scheuble, E.J. Windhab, and P. Fischer

ETH Zürich, Institute of Food, Nutrition and Health, Schmelzbergstrasse 9, 8092 Zürich, Switzerland

Received 16 April 2013 / Received in final form 23 April 2013
Published online 17 June 2013

Abstract. The static and dilatational response of β-lactoglobulin fibrils and native β-lactoglobulin (monomers) at water-air and water-oil interfaces (pH 2) was measured using the pendant drop method. The resulting adsorption behavior and viscoelasticity is dependent of concentration and adsorption time. The interfacial pressure of the β-lactoglobulin fibrils obtained in static measurements was 16–18 mN/m (against air) and 7 mN/m (against oil) for all concentrations. With higher concentrations, faster adsorption kinetics and slightly higher interfacial and surface pressure is achieved but did not lead to higher viscoelastic moduli. The transient saturation of the interface is similar for both the fibril solution and the monomers, however the fibril solution forms a strong viscoelastic network. To evaluate the superimposed adsorption behavior and rheological properties, the formed interfacial layer was subjected to dilatational experiments, which were performed by oscillating the surface area of the drop in sinusoidal and sawtooth (diagonal) deformation manner. The sinusoidal oscillations (time depended area deformation rate) result in a complex interfacial tension behavior against air and oil interfaces and show remarkable differences during compression and expansion as emphasized by Lissajous figures. For diagonal (constant area deformation rate) experiments, a slight bending of the interfacial tension response was observed at low frequencies emphasizing the influence of protein adsorption during rheological measurements.

1 Introduction

Interfacial rheology can be performed by either deforming or stressing a defined area (interfacial shear rheology) or by applying area variations, which is called dilatational interfacial rheology [1]. Several methods are available to measure dilatational rheology, which are based on Langmuir trough [2] and pendant drop tensiometer techniques [3]. Dilatational rheology is used to understand phenomena occurring at interfaces, where the surface is prone to change during emulsion and foam generation [4,5]. The stabilizing surface active material can be either proteins [6], small weight molecular surfactants [7], particles [8] or a combination of the previously mentioned [9]. Overviews on the rheological behaviors of various surface active molecules

[a] e-mail: patrick.ruehs@hest.ethz.ch

are extensively presented by Sagis [10] and Erni [11]. Protein stabilized interfaces are especially interesting due to the build up of viscoelastic layers [12–15]. Most of the protein fraction is irreversibly adsorbed at the interface, leading to formation of wrinkles at the water-oil interface after shape oscillation and generally form multilayer films rendering the use of interfacial rheological models into an extremely challenging issue [6,10,16]. Both phenomena complicate the data analysis, as the second and third layer could easily adsorb upon expansion, making it difficult to predict to what extend the surface dilatational parameters can be accounted for, either adsorption or relaxation effects or a combination of both.

One of the most widely studied protein at various interfaces is β-lactoglobulin due to its high relevance in the food industry [17–20]. This protein can form self-assembly fibrillar structures under denaturing conditions and have been thoroughly studied during the last few years [21–27]. Different processing conditions and modifications can make these fibrils shorter [23], thicker [28] or flexible [25]. Recent studies, focussing on interfacial activity and shear rheology of heat-induced fibrils showed the adsorption behaviour of fibrils at water-oil interfaces [23,29,30]. Dilatational experiments were however not performed. Using these fibrils as model molecules for semi-flexible rods at interfaces might provide new opportunities to develop models explaining adsorption and relaxation mechanisms of proteins at interfaces as well as isotropic-nematic phase transitions.

Recent publications have critiqued the use of the pendant drop method. The difference between rheological response and protein adsorption is not easy to distinguish and under these conditions dilatational data can be difficult to interpret [31,32]. In addition, the effect of viscous forces on interfacial tension may also interfere when performing measurements with the pendant drop [33]. So, the pendant drop method, originally developed for surfactants, does not seem suitable for proteins, as they differentiate greatly from surfactants and form complex structures at the interface, leading to a gel like formation i.e. rendering the system from surface tension to surface elasticity governed [1,11,12,15]. To highlight this shortcoming, β-lactoglobulin fibrils at pH 2 were investigated on their kinetic adsorption and dynamic behavior at the water-oil and water-air interface. Comparative measurements were performed with native β-lactoglobulin (referred to as monomers) at pH 2. Sinusoidal (time depended area deformation rate) and diagonal (constant area deformation rate) oscillations were imposed to the adsorption layer to study the change of the dilatational stress response and therefore the different ratios of adsorption and rheological processes.

2 Materials and methods

2.1 Materials

For this study β-lactoglobulin fibrils were produced as mentioned in literature [22]. After the denaturation process at 90 °C for 5 hours at pH 2 of a 2w/w% water solution, long fibrils are formed [22,34]. During fibril synthesis 75% of the original protein solution is converted into fibrils. The remaining 25%, peptides and monomers, stay in solution and were dialyzed out of the solution [22,23]. The formed fibrils, checked by Atomic Force Microscopy, have a diameter of 2–10 nm and an average contour length of 2–4 μm as reported in literature [34]. These fibrils were tested for their dilatational properties at the water-oil and water-air interface. In total four different concentrations (0.01, 0.03, 0.05 and 0.09w/w%) of β-lactoglobulin fibrils were measured. Additionally, measurements with β-lactoglobulin monomers at pH 2 at a concentration of 0.01w/w% were performed against both interfaces. The β-lactoglobulin monomer solution was prepared by dissolving β-lactoglobulin

(Davisco Foods Inc.) at the desired concentration in MilliQ water and then changed to pH 2. As the oil phase, MCT Oil (Delios GmbH) was used to facilitate comparisons to an earlier publication [23,30]. The oil was used as received after having checked the interfacial tension development against water decreased a maximum of 0.5 mN/m after one hour of adsorption. Protein adsorption causes a faster decrease in tension, so that the small decrease in tension can be neglected.

2.2 Methods

To determine the dilatational parameters, a pendant drop tensiometer equipped with a needle of 1.96 mm diameter (PAT-1, Sinterface Technologies, Germany) was used. The setup and the methodology is described elsewhere [35]. Static interfacial tension and surface tension measurements are performed by leaving the volume of the drop constant. The drop contour is monitored and fitted to the Young-Laplace equation. This method allows the measurement of adsorption kinetics of the surface active material. The difference between the surface tension of the pure solvent γ_0 and the surface tension $\gamma(t)$ of the solution at a specific time t is defined as surface pressure $\pi(t)$.

$$\pi(t) = \gamma_0 - \gamma(t). \tag{1}$$

For simplicity reasons, the surface tension and interfacial tension will be referred to as interfacial tension γ for both the water-air and water-oil interface. To aid discussions later, a small summary of the involved equations are presented. If an interface at its equilibrium is disturbed by expansion or compression, i.e. by an area change dA, the elastic modulus E is given by Gibbs equation:

$$E = \frac{d\gamma}{dA/A} \tag{2}$$

where γ is the interfacial tension and A the total interfacial area. During dynamic measurements the area change dA is performed periodically. The pendant drop tensiometer increases and decreases the area harmonically. The following equations describe the harmonic expansion/compression of the interfacial area A with the frequency ω and the resulting oscillation of the interfacial tension γ, due to adsorption layer at the interface to be expanded and compressed:

$$A = A_0 + \Delta A \sin(\omega t) \tag{3}$$

$$\gamma = \gamma_0 + \Delta\gamma \sin(\omega t + \theta). \tag{4}$$

The interfacial tension responds with the same frequency ω but with a phase shift θ [36]. The resulting viscoelastic modulus $E^* = E' + iE''$ is a complex number with a real part E' (storage modulus) and an imaginary part E'' (loss modulus).

Using the following equations both moduli E' and E'' can be determined through a Fourier transformation of the measured data [37]:

$$E' = \Delta\gamma \frac{A_0}{\Delta A} \cos\theta \tag{5}$$

$$E'' = \Delta\gamma \frac{A_0}{\Delta A} \sin\theta. \tag{6}$$

For a small harmonic perturbation of interfacial area, the interfacial tension response is directly related to the surface dilatational viscoelasticity [36]. To determine the

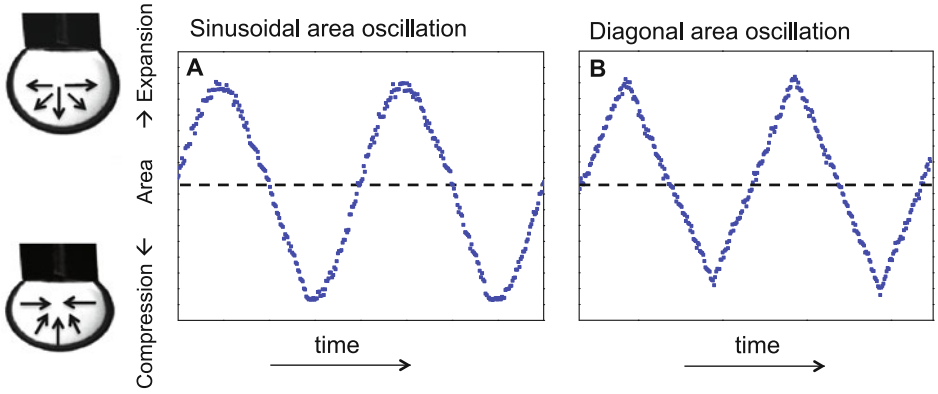

Fig. 1. Dynamic frequency measurements performed with the pendant drop method. The influence of expansion and compression on the drop is shown on the left. A) Sinusoidal oscillation against time. B) Diagonal oscillation against time.

amplitude necessary for the dynamic measurements, dilatational amplitude sweep were performed. After equilibration of the drop (12 mm^3) for 12 hours, the area was varied (0.7 to 7.1%) at a constant frequency of (0.01 Hz) to determine the linear viscoelastic regime. Before each area amplitude change, i.e. constant increase of the drop size, the drop was left constant for 20 minutes. After determining the suitable amplitude, dynamic frequency measurements were performed. Every measurement starts with a equilibration time of 12 hours, followed by sinusoidal oscillation sequences (time dependent area deformation rate, see Fig. 1A) from 0.1 to 0.001 Hz of at least 8 periods. Between each sequence a lag of 20 minutes for equilibration was introduced to allow the drop to stabilize. To monitor the influence of superimposed adsorption on the oscillation signal, diagonal oscillations (constant area deformation rate, see Fig. 1B) at the same frequencies were performed. All experiments were performed at 20 °C.

3 Results and discussion

3.1 Adsorption of β-lactoglobulin fibrils and monomers at the water-air and water-oil interface

Figure 2A shows the adsorption kinetics of the three different concentrations of the β-lactoglobulin fibrils. The three lower curves (filled symbols) show the concentrations against oil and the top three against air. An increase in interfacial pressure can be observed with increasing concentration. The pressure reached a a steady value after 12 hours of 16–18 mN/m (against air) and 7 mN/m (against oil) (see Fig. 2B). The adsorption rate (slope of interfacial pressure over time) is higher at the water-air surface than at the water-oil interface. The interfacial pressure difference between water-air and water-oil is in accordance with data reported in literature [3].

In comparison, solutions of β-lactoglobulin monomers at pH 2 showed a different adsorption behavior at both interfaces. In particular, the pressure increases slower in comparison to the fibril solution (see Fig. 3). This is not too surprising, since the monomer, being the protein in its natural form, still has to unfold at the interface. The adsorption/denaturing kinetics of most proteins follow a three domain system: At first the proteins adsorbs at the interface, causing a rapid increase in interfacial pressure. Then they denature and in a final step slowly rearrange. A complete steady

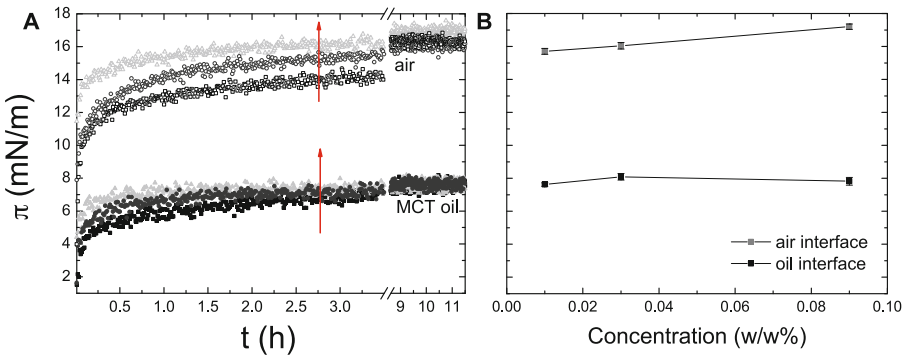

Fig. 2. A) The surface and interfacial pressure is plotted against time of three concentrations of β-lactoglobulin fibrils at pH 2 (from dark grey to light grey: 0.01 (squares), 0.03 (circles), and 0.09 w/w% (triangles)) at the water-air and water-oil interface. The arrows indicate the concentration increase to higher concentrations. B) Three steady state values of concentration (w/w%) and pressure of β-lactoglobulin fibrils at the water-air and water-oil interface at pH 2 after 12 h.

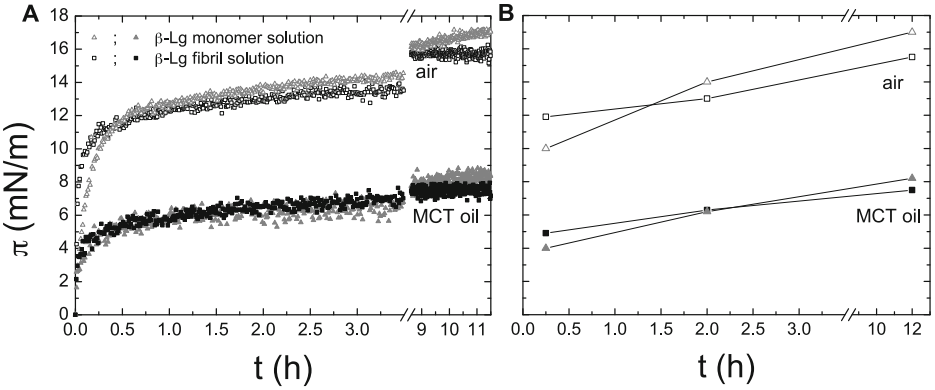

Fig. 3. A) The surface pressure is plotted against time of β-lactoglobulin fibrils (squares) and β-lactoglobulin monomers (triangles) at a concentration of 0.01 w/w% and at pH 2 against oil (closed symbols) and against air (open symbols). B) The interfacial pressure of β-lactoglobulin fibrils (squares) and β-lactoglobulin monomers (triangles) at the water-air and water-oil interface after 0.25, 2 and 12 hours.

state situation for protein adsorption can take up to several days [38]. The fibrils, being already denatured through the heating step, might not undergo the second denaturation step. Although the increase in surface and interfacial pressure is slower at the beginning, the steady state value of the β-lactoglobulin monomers after 12 hours is higher than that of the β-lactoglobulin fibrils (see Fig. 3B). The surface coverage of the β-lactoglobulin monomers is higher than the β-lactoglobulin fibrils after reaching the steady state due to closer packing. After 12 hours the interfacial pressure is stable, so that the dilatational experiments were performed after this period (see next chapter).

3.2 Dilatational amplitude sweep

Before performing the oscillatory frequency sweep experiments, amplitude sweeps at different area deformations (strains) were performed. The applied strain corresponds

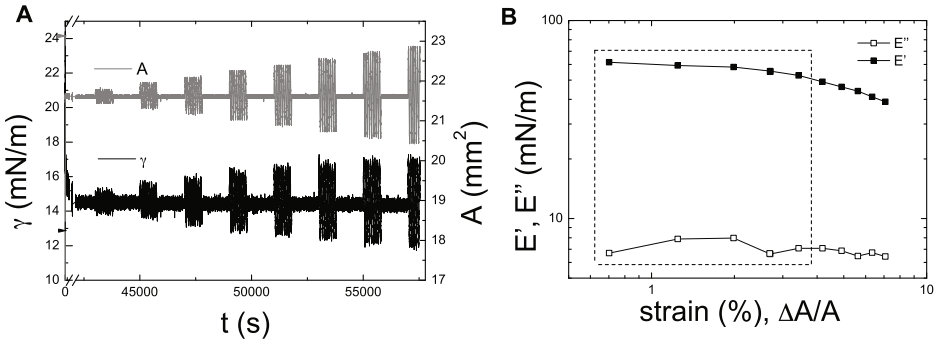

Fig. 4. A) The interfacial tension of β-lactoglobulin fibrils (0.01 w/w%, pH 2) at the water-oil interface is plotted against the time. After 12 hours of equilibration (t = 43200 s) the drop area was sinusoidally oscillated at a frequency of 0.01 Hz with area amplitudes from 0.7 to 7.1%. B) The calculated moduli E' (filled squares) and E'' (empty squares) of the dilatational amplitude sweep as a function of strain. The lines are to guide the eye. The dotted box represents the linear regime.

to $\Delta A/A$. As depicted in Fig. 4, the linear regime is limited to an amplitude of around 5%. We set our value to 2.7% to stay in the linear regime. At 1% and lower, the dilatational parameters can not be calculated due to instrument restrictions. Ravera et al. claims that for deformations below 10% the regime is per se linear [36], while Freer et al. chose amplitudes below 3% to avoid non-linear effects [39,40]. Our measurements additionally show that although the elastic modulus E' can be nicely determined, the viscous modulus E'' values are not constant in the linear regime. In contrast to Loglio et al. [41] our values for E' and E'' show a high dependency on the set amplitude. We propose that this is strictly dependent on the material used and amplitude sweeps should therefore be routinely performed in addition to frequency sweeps as done in bulk and interfacial shear rheology. Additionally, this might be important in future experiments, due to the high importance given lately to the non-linear regime in shear rheology [42,43].

That a properly chosen strain rate is a crucial parameter, is supported in Fig. 5, where a constant increase of interfacial area over a defined time was performed for a single drop (0.01w/w% β-lactoglobulin fibrils) in oil. In region I, the interfacial tension increase is constant due to the reduced amount of adsorbed molecules per unit area as the short time frame did not allow adsorption of proteins. In region II the area increase and the allowed time for adsorption allowed protein adsorption to occur and thus the slope of interfacial tension starts to diminish. At a certain time/area change, the interfacial tension peaks (see region III) and after the maximum is reached, the value begins to decrease and level out after long time (see region IV) due to additional adsorption. This measurement highlights the importance of the chosen area change per time as adsorption can corrupt the signal even at fairly low area changes.

3.3 Sinusoidal and diagonal oscillations of β-lactoglobulin fibrils

To study the superposition of adsorption and dilatation, sinusoidal and diagonal oscillations were performed. First, the drop area was left constant for 12 hours during adsorption. After adsorption the drop was oscillated by imposing a sinusoidal (12 h $\leq$ t $\leq$ 17) and a diagonal (17 h $\leq$ t $\leq$ 25 h) area variation as depicted in Fig. 6. Six oscillation frequencies were performed for each concentration of β-lactoglobulin fibrils. Between each oscillation procedure, the area was left constant for 20 minutes

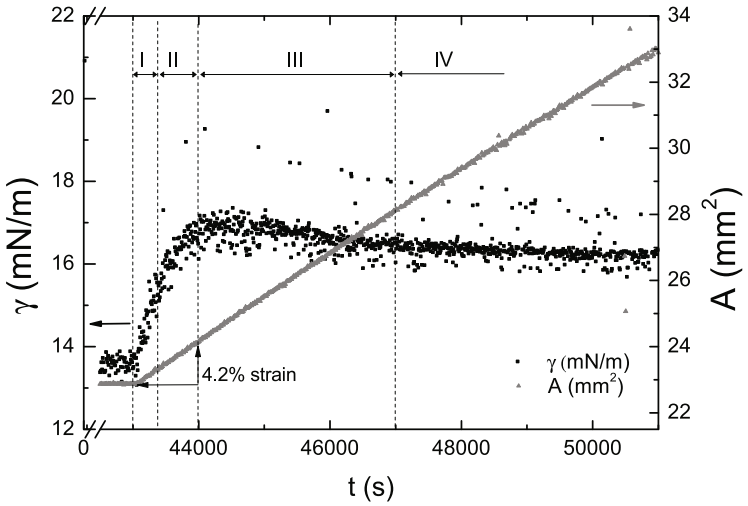

Fig. 5. After 12 hours of equilibration (t = 43000 s), the drop (0.01w/w% β-lactoglobulin fibrils) was constantly increased (2.6% / 400 s) in interfacial drop area. Different regions are marked as the strain amplitude in comparison to the starting strain. Region I represents the strain up to 1.8%, II = 4.2%, III = 16%, and IV the remaining constant adsorption period.

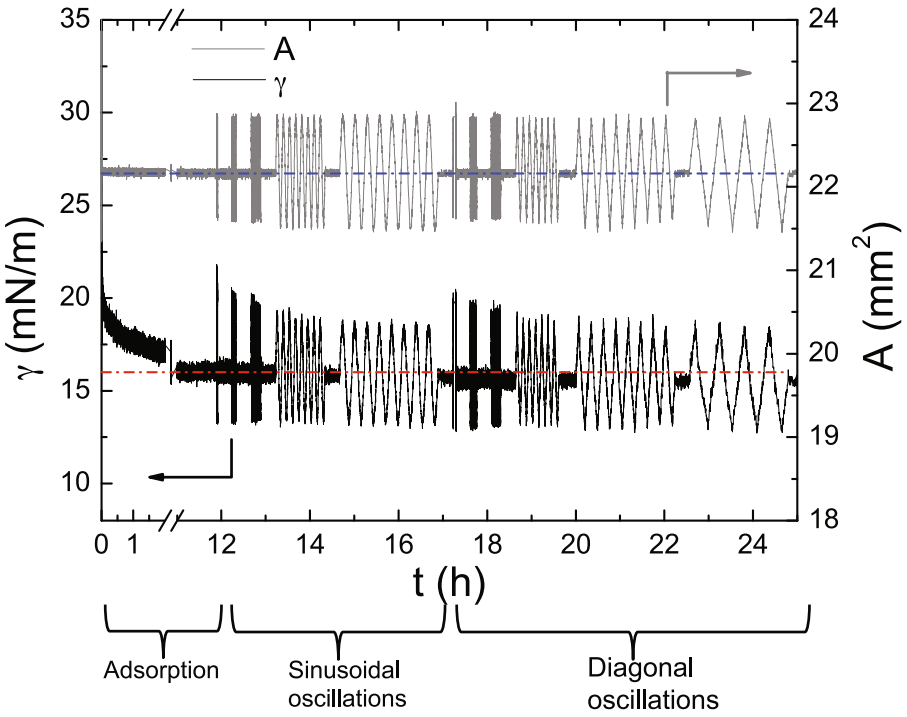

Fig. 6. Exemplary frequency sweep, including the adsorption period (up to t = 12 h), sinusoidal oscillation (12 h $\leq$ t $\leq$ 17 h), and diagonal oscillation (17 h $\leq$ t $\leq$ 25 h). The area (grey) and the interfacial tension (black) is plotted as a function of time.

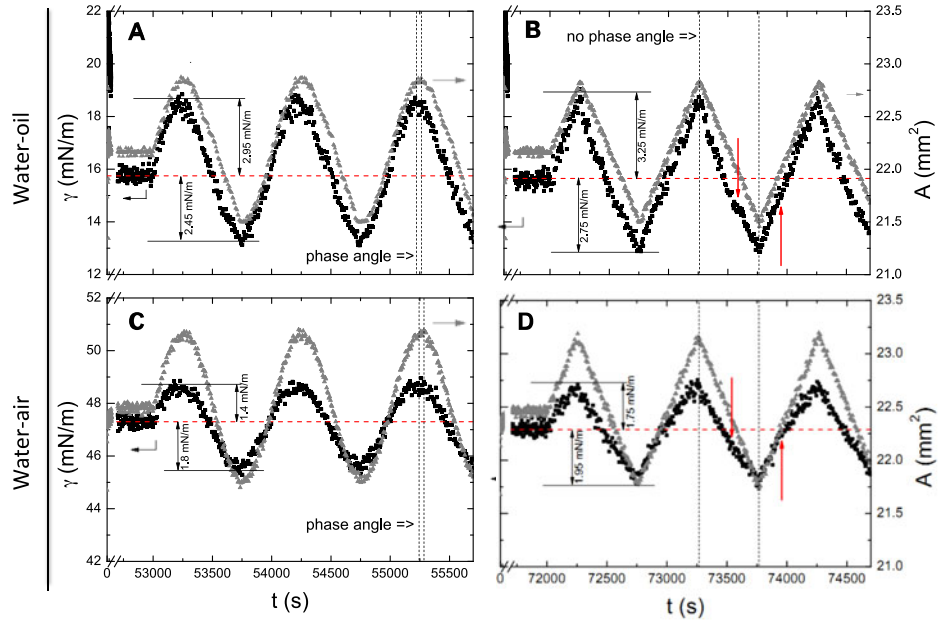

Fig. 7. Interfacial tension during area A oscillations after adsorption ($t \leq 43200$ s) of 0.01 w/w% β-lactoglobulin fibril at a frequency of 0.001 Hz. Sinusoidal (A) and diagonal (B) oscillation of the water-oil interface. Sinusoidal (C) and diagonal (D) oscillations at the water-air interface.

to equilibrate. Comparing the compression cycles (see Fig. 6) for all oscillations frequencies, the maximal amplitude of the responding interfacial tension is frequency independent. Contrary to the compression, the expansion cycle causes the tension amplitude to vary from high values at high frequencies and low values at lower frequencies. At low frequencies an adsorption effect might take place additionally to the surface relaxation effects. This effect is more pronounced against air than against oil. After each oscillation sequence, the interfacial tension is lower than the value before oscillation through rearrangements and adsorption effects. This effect is more pronounced after lower frequency oscillations indicating the superposition of adsorption (slow process) and dilatational measurements (frequency dependent).

Focussing on a few deformation cycles only, it becomes clear that the interfacial tension amplitude of β-lactoglobulin fibrils at the same concentration (0.01w/w%) and frequency (0.001 Hz) differs largely for air or oil interface (see Fig. 7A and C). Against oil, Fig. 7A, the amplitude to the top is higher (2.95 mN/m) than to the bottom (2.45 mN/m) in comparison to the starting equilibration interfacial tension value. Against air, Fig. 7C, the amplitude at compression is higher (1.8 mN/m) than at expansion (1.4 mN/m). During the diagonal area variations the amplitude interfacial tension response is comparable with the sinusoidal interfacial tension response (see Fig. 7B and D). This effect shows the protein adsorption interfering with the flow induced relaxation mechanism in the interface. The reason for this could be that the adsorption effect is not as predominant against the oil phase as at the air interface. As observed in Fig. 6, the amplitude during compression is independent of frequency. This shows that a certain amount of protein is irreversibly adsorbed at the interface and superimpose rheological data.

The sinusoidal oscillatory data were used to calculate E' and E'' (Fig. 8) for both the oil and air interface. The formed adsorption layer at the oil phase is more elastic

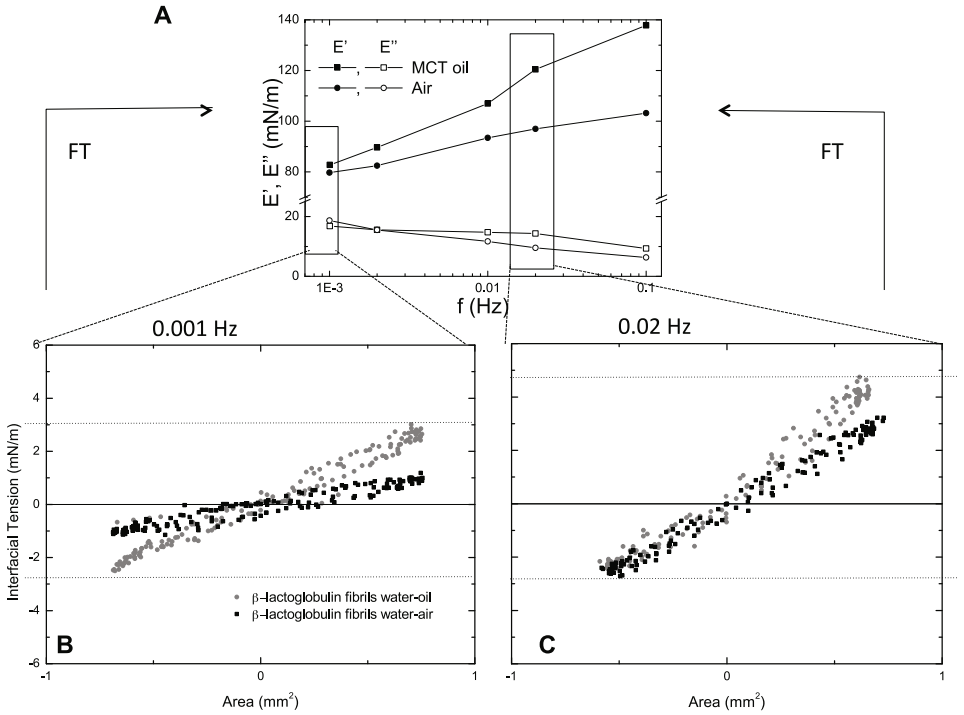

Fig. 8. A) Interfacial elastic E' and viscous E'' moduli of air and MCT oil with 0.01w/w% β-lactoglobulin fibril solutions a function of frequency f at a strain of 2.7%. The lines are to guide the eye. B) The interfacial tension of β-lactoglobulin fibril at the water-oil and water-air surface is plotted against the drop area for a oscillation at 0.001 Hz. C) The interfacial tension of β-lactoglobulin fibril at the water-oil and water-air surface is plotted against the drop area of one sole oscillation at 0.02 Hz. The line represents the dynamic equilibrium interfacial tension used for the calculation of E' and E''. The dotted lines in both graphs represent the maximum interfacial tension response of the interface of each oscillation. By Fourier transformation (FT) the interfacial elastic E' and viscous E'' moduli of air and MCT oil with 0.01w/w% β-lactoglobulin fibril solutions a function of frequency f at a strain of 2.7% are calculated.

than the layer at the air through hydrophobic interactions of the protein with the oil as reported e.g. by Clark et al. [16]. In our case, the water-oil interface is more elastic than the water-air interface. Other authors have seen contrary effects, but this is mainly dependent on concentration and protein-type [3]. The square boxes in Fig. 8 at 0.001 and 0.02 Hz mark the frequencies discussed in Fig. 8B and C. The moduli E' and E'' of the 0.001 Hz box are from the sinusoidal oscillations in Fig. 7A and C. Although the difference between the amplitudes is up to 25%, the calculated moduli are robust and inside the typical error range of the Fourier transformation data. To emphasize the different oscillation responses, the interfacial and surface tensions are plotted against the area change and the resulting Lissajous figures (each out of one oscillation cycle) are depicted in Fig. 8B and C. At frequencies of 0.001 and 0.02 Hz the interfacial and surface tension amplitudes vary greatly. At high and low frequencies, the film seems to oscillate around a different mean interfacial tension as pointed out by the dotted lines. The lines represent the real starting interfacial tension value. This shift shows that the dynamic equilibrium is not the same as the starting equilibrated value. E' and E'' can still be calculated and give a qualitative result, however to really compare different expansion and compression behavior, in this case against oil and

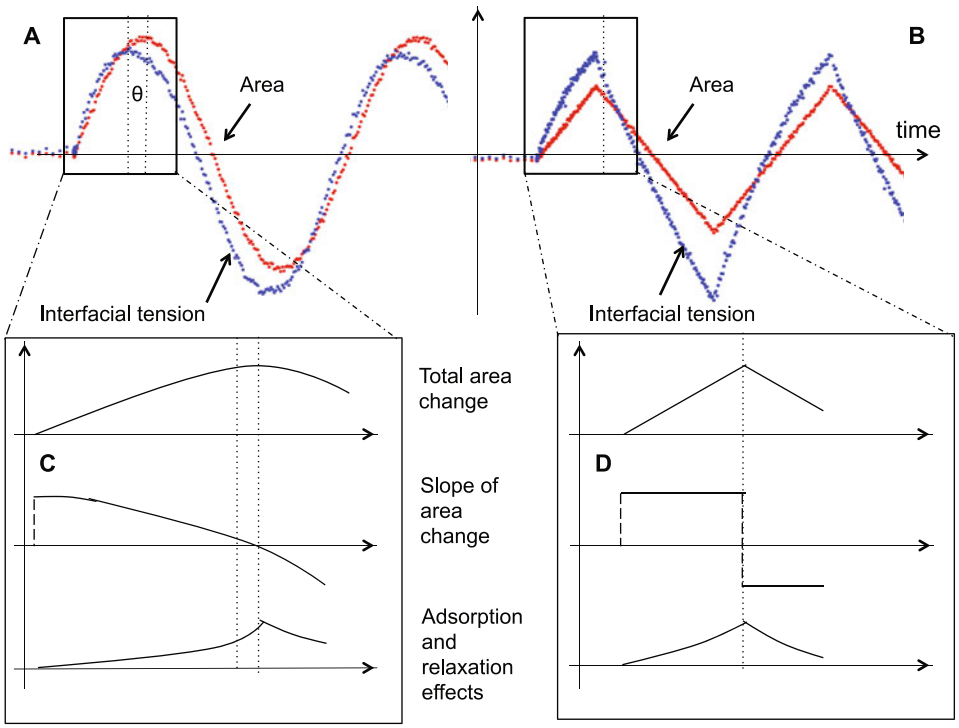

Fig. 9. A) Interfacial tension during area sinusoidal oscillations after adsorption of 0.01w/w% β-lactoglobulin fibrils. B) Interfacial tension during diagonal oscillations after adsorption of 0.01w/w% β-lactoglobulin fibrils. The slope of the area change for sinusoidal (C) and diagonal (D) oscillations is shown.

air, a different approach is needed. This questions the validity of the used method, since it does not differentiate between the compression and expansion amplitude. We suggest that a clear differentiation is needed to compare similar moduli.

In the sinusoidal oscillation shown in Fig. 7 the interfacial tension data precedes the area curve, made clear by Fig. 9A. Initially the surface area change per time is high (Fig. 9C). The total free area (without adsorbed molecules) is at this time low, leading to a rise in interfacial tension due to a lower amount of adsorbed molecules. The subsequent adsorption processes (either in-interface or adsorption from bulk) at the interface causes a decrease in tension. At a later stage the area change per time is small, which leads to a faster adsorption of proteins and/or relaxation of the interface than the area change. This causes the interfacial tension to reach the maximum before the area, as depicted by the phase angle. The phase angle can thus be explained by adsorption and relaxation processes. A variety of surface phenomena play a role in different time scales. Diffusion from the bulk phase, relaxation in the interface, but also retardation of adsorption through sterical hindrance, reorientation after adsorption and phase transitions might cause this behavior [1,2,44,45]. The observed positive phase angle was reported in other publications [46–48], however a negative phase angle (where the tension lags behind the area) has also been observed in other publications [36,48]. In our measurements the tension is nearly in phase with the area change at high frequencies and out of phase at low frequencies. This effect is also dependent on the set area amplitude. The higher phase angle at the water-air interface can be explained by the faster adsorption to the air interface. The phase

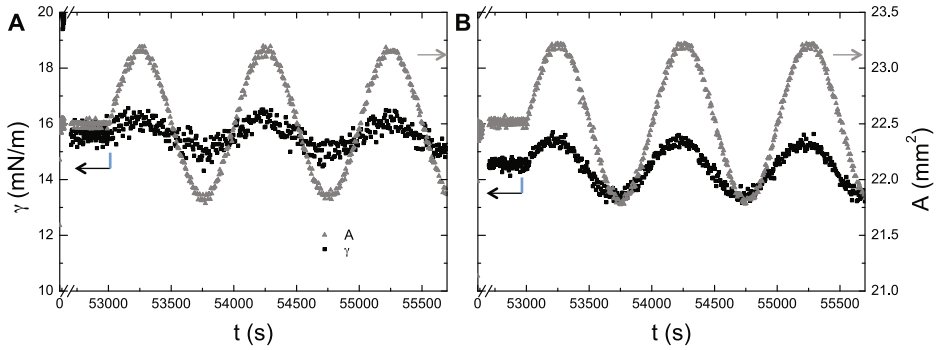

Fig. 10. Interfacial tension during area A sinusoidal oscillation at a frequency of 0.001 Hz and a strain of 2.7% at the water-oil (A) and water-air (B) interface.

angle is present at the water-air (high phase angle) and water-oil (low phase angle) interface.

The phase angle is characteristic of sinusoidal oscillations, caused by the changing slope of the area function (Fig. 9D). In the diagonal oscillation shown in Fig. 7 the interfacial tension data does not precede the area curve. In diagonal oscillations (Fig. 9B) a different effect can be observed. The response interfacial tension shows a slight bend. Already at frequencies below 0.01 Hz a bend in the interfacial tension can be observed. The bend is only visible at low frequencies and thus not of protein nature, but caused by adsorption/relaxation effects. This effect however underlines the strong evidence that adsorption plays a major role in this process, due to it's time dependance. This bend of the response function was already observed in an earlier study where the effect was said to be of protein intrinsic nature [49]. The authors argue that the bend is caused by conformational changes of the proteins during expansion and compression.

3.4 Sinusoidal oscillations of β-lactoglobulin monomers at a concentration of 0.01 w/w%

To compare the β-lactoglobulin monomers with the β-lactoglobulin fibrils, both systems were analyzed after the same adsorption time, concentration, pH, amplitude and frequencies. The β-lactoglobulin monomers, in comparison to the fibrils, exhibit a weak interfacial tension response function (see Fig. 10) and do not build up a strong viscoelastic layer. Both systems, monomers and fibrils, being at pH 2 and at the same interfacial pressure (Fig. 3) should electrostatically repel each other [23,50]. The observed difference can be explained by the fibril morphology which leads to an increased viscoelasticity through steric effects.

3.5 Dilatational viscoelasticity of β-lactoglobulin fibrils

Although the analysis is corrupted by the superimposed adsorption, the dilatational viscoelasticity can be calculated. The dilatational viscoelasticity E^* of β-lactoglobulin fibrils at the water-oil (A) and water-air (B) interface four different concentrations and frequencies is plotted in Fig. 11. Starting at low concentrations, the dilatational viscoelasticity increases until a maxing value is reached. This maximum dilatational viscoelasticity is slightly different for water-air interfaces than for water-oil interfaces

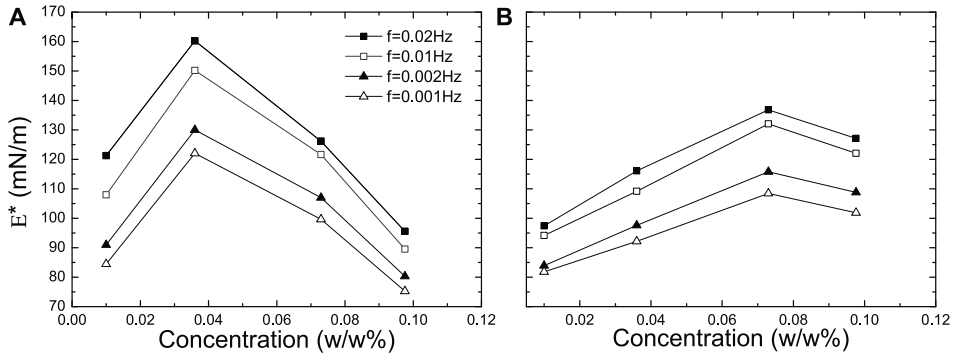

Fig. 11. Dilatational viscoelastic modulus E^* of β-lactoglobulin fibrils at pH 2 at the water-oil (A) and water-air (B) interface as a function of concentration at different frequencies f and a strain of 2.7%. The lines are to guide the eye.

as reported previously for polyelectrolytes and proteins [3,51]. At higher concentrations the conformation of proteins at the interface can be considered as not ideal because of jamming and non-ideal alignment during adsorption: The maximum of E^* indicates the best packing organization of the β-lactoglobulin fibrils at the interfaces. The highest viscoelastic properties of β-lactoglobulin fibrils is therefore not dependent on the static interfacial pressure but on the elastic properties of the formed network.

4 Conclusion

We have investigated the dilatational rheology of β-lactoglobulin fibrils and the corresponding native protein (monomers) both at pH 2 at the water-air and water-oil interface. The pressure reached through the static measurements is 16–18 mN/m (against air) and 7 mN/m (against oil). With higher concentrations a faster adsorption kinetics are achieved but do not lead to a higher viscoelastic modulus of the β-lactoglobulin fibrils. Both the fibril solution and the monomers saturate the interface similarly, however only the fibril solution forms a strong viscoelastic network. To evaluate the superposition of protein fibril adsorption and dilatational rheology, the interfacial layer was subjected to sinusoidal and diagonal dilatational experiments. The sinusoidal oscillations showed that for area expansion different interface and surface tensions can be observed. The compression amplitudes however remain constant and are independent of frequency. We used Lissajous figures to show the strong differences of the interfacial tension differences at water-oil and water-air interfaces. Additionally to the sinusoidal oscillations, diagonal oscillations were performed, where the interfacial tension function showed a bend in the response function. This effect was shown to be time dependent, as the bend was not observed at high frequencies. All experiments provide evidence that protein adsorption is interfering with rheological properties and that new measuring techniques and models have to be developed to understand adsorption and relaxation phenomena occurring at interfaces during dynamic measurements.

We would like to express our thanks to Annekathrin Mütze and Varvara Mitropoulos for their valuable input. The authors thank Raffaele Mezzenga for providing the fibrils. PR acknowledges financial support by ETH Zurich (Project ETHIIRA TH 32-1 “Amyloid Protein Fibers at Surfaces and Interfaces”).

References

1. M.A. Bos, T. van Vliet, Adv. Coll. Interf. Sci. **3**, 437 (2001)
2. D Graham, M. Phillips, J. Coll. Interf. Sci. **76**, 227 (1980)
3. J. Benjamins, A. Cagna, E. Lucassen-Reynders, Coll. Surf. A: Physicochem. Eng. Aspects **114**, 245 (1996)
4. P Wierenga, H. Gruppen, Coll. Surf. A: Physicochem. Eng. Aspects **15**, 365 (1996)
5. B.S. Murray, E. Dickinson, Y. Wang, Food Hydrocolloids **23**, 1198 (2009)
6. E.M. Freer, K.S. Yim, G.G. Fuller, C.J. Radke, Langmuir **20**, 10159 (2004)
7. V. Fainerman, S. Lylyk, E. Aksenenko, J. Petkov, J. Yorke, R. Miller, Coll. Surf. A: Physicochem. Eng. Aspects **354**, 8 (2010)
8. E. Dickinson, Curr. Opinion Coll. Interf. Sci. **15**, 40 (2010)
9. V. Pradines, J. Krägel, V.B. Fainerman, R. Miller, J. Phys. Chem. B **113**, 745 (2009)
10. L.M.C Sagis, Rev. Mod. Phys. **83**, 1367 (2011)
11. P. Erni, Soft Matter **7**, 7586 (2011)
12. P. Erni, P. Fischer, E.J. Windhab, Appl. Phys. Lett. **87**, 244104 (2005)
13. P. Erni, P. Fischer, Curr. Opinion Coll. Interf. Sci. **12**, 196 (2007)
14. P. Erni, P. Fischer, V. Herle, M. Haug, E.J. Windhab, Chem. Phys. Chem. **9**, 1833 (2008)
15. P. Erni, E.J. Windhab, P. Fischer, Macromolec. Mater. Eng. **296**, 249 (2011)
16. D.C. Clark, A.R. Mackie, P.J. Wilde, D.R. Wilson, Faraday Discuss. **98**, 253 (1994)
17. J.T. Petkov, T.D. Gurkov, B.E. Campbell, R.P. Borwankar, Langmuir **16**, 3703 (2000)
18. M.H. Lee, D.H. Reich, K.J. Stebe, R.L. Leheny, Langmuir **26**, 2650 (2010)
19. E. Kolodziejczyk, V. Petkova, J.-J. Benattar, M.E. Leser, M. Michel, Coll. Surf. A: Physicochem. Eng. Aspects **279**, 159 (2006)
20. A.I. Romoscanu R. Mezzenga, Langmuir **21**, 9689 (2005)
21. O.G. Jones R. Mezzenga, Soft Matter **8**, 876 (2012)
22. J.M. Jung, G. Savin, M. Pouzot, C. Schmitt, R. Mezzenga, Biomacromolecules **9**, 2477 (2008)
23. J.M. Jung, D.Z. Gunes, R. Mezzenga, Langmuir **26**, 15366 (2010)
24. C. Lara, I. Usov, J. Adamcik, R. Mezzenga, Phys. Rev. Lett. **107**, 238101 (2011)
25. S. Jordens, J. Adamcik, I. Amar-Yuli, R. Mezzenga, Biomacromolecules **12**, 187 (2011)
26. C. Li, J. Adamcik, R. Mezzenga, Nat Nano **7**, 421 (2012)
27. S. Bolisetty, J.J. Vallooran, J. Adamcik, S. Handschin, F. Gramm, R. Mezzenga, J. Coll. Interf. Sci. **361**, 90 (2011)
28. C. Lara, J. Adamcik , S. Jordens , R. Mezzenga, Biomacromolecules **12**, 1868 (2011)
29. L. Isa, J.M. Jung, R. Mezzenga, Soft Matter **7**, 8127 (2011)
30. P.A. Rühs, N. Scheuble, E.J. Windhab, R. Mezzenga, P. Fischer, Langmuir **34**, 12536 (2012)
31. A. Yeung, T. Dabros, J. Masliyah, Langmuir **13**, 6597 (1997)
32. A. Yeung, L. Zhang, Langmuir **22**, 693 (2006)
33. E.M. Freer, H. Wong, C. Radke, J. Coll. Interf. Sci. **282**, 128 (2005)
34. J. Adamcik, J.M. Jung, J. Flakowski, P. De Los Rios, G. Dietler, R. Mezzenga, Nature Nanotechnol. **5**, 423 (2010)
35. G. Loglio, P. Pandolfini, R. Miller, A. Makievski, F. Ravera, M. Ferrari, L. Liggieri, *Novel Methods to Study Interfacial Layers* (Elsevier, 2001), p. 439
36. F. Ravera, G. Loglio, V.I. Kovalchuk, Curr. Option Coll. Interf. Sci. **15**, 217 (2010)
37. L.G. Cascão Pereira, O. Théodoly, H.W. Blanch, C.J. Radke, Langmuir **19**, 2349 (2003)
38. C. Beverung, C. Radke, H. Blanch, Biophys. Chem. **81**, 59 (1999)
39. E.M. Freer, T. Svitova, C.J. Radke, J. Petrol. Sci. Eng. **39**, 137 (2003)
40. E.M. Freer, C.J. Radke, J. Adhes. **80**, 481 (2004)
41. G. Loglio, P. Pandolfini, R. Miller, A.V. Makievski, J. Krägel, F. Ravera, B.A. Noskov, Coll. Surf. A: Physicochem. Eng. Aspects **261**, 57 (2005)
42. R.H. Ewoldt, C. Clasen, A.E. Hosoi, G.H. McKinley, Soft Matter **3**, 634 (2007)
43. P. Erni, A. Parker, Langmuir **28**, 7757 (2012)
44. G. Serrien, G. Geeraerts, L. Ghosh, P. Joos, Coll. Surf. **68**, 219 (1992)

45. M. van den Tempel, E. Lucassen-Reynders, Adv. Coll. Interf. Sci. **18**, 281 (1983)
46. R. Wustneck, P. Enders, N. Wustneck, U. Pison, R. Miller, D. Vollhardt, Phys. Chem. Comm. **2**, 50 (1999)
47. A. Laza-Knoerr, N. Huang, J.-L. Grossiord, P. Couvreur, R. Gref, J. Incl. Phenom. Macro. Chem. **69**, 475 (2011)
48. Z. Wang, G. Narsimhan, Langmuir **21**, 4482 (2005)
49. P. Chen, R. Prokop, S. Susnar, A. Neumann, *Proteins at Liquid Interfaces, Studies in Interface Science* (Elsevier, 1998), p. 303
50. S. Roth, B.S. Murray, E. Dickinson, J. Agricultural and Food Chem. **48**, 1491 (2000)
51. F. Monroy, F. Ortega, R.G. Rubio, *Surface rheology studies of spread and adsorbed polymer layers* (Koninklijke Brill NV, 2009), p. 179